Proc. IAHS, 371, 99–107, 2015
proc-iahs.net/371/99/2015/
doi:10.5194/piahs-371-99-2015

Wind effects on leaf transpiration challenge the concept of "potential evaporation"

S. J. Schymanski and D. Or

Swiss Federal Institute of Technology, Zurich, Switzerland

Correspondence to: S. Schymanski (stan.schymanski@env.ethz.ch)

Received: 11 March 2015 – Accepted: 11 March 2015 – Published: 12 June 2015

Abstract. Transpiration is commonly conceptualised as a fraction of some potential rate, driven by so-called "atmospheric evaporative demand". Therefore, atmospheric evaporative demand or "potential evaporation" is generally used alongside with precipitation and soil moisture to characterise the environmental conditions that affect plant water use. Consequently, an increase in potential evaporation (e.g. due to climate change) is believed to cause increased transpiration and/or vegetation water stress. In the present study, we investigated the question whether potential evaporation constitutes a meaningful reference for transpiration and compared sensitivity of potential evaporation and leaf transpiration to atmospheric forcing. A physically-based leaf energy balance model was used, considering the dependence of feedbacks between leaf temperature and exchange rates of radiative, sensible and latent heat on stomatal resistance. Based on modelling results and supporting experimental evidence, we conclude that stomatal resistance cannot be parameterised as a factor relating transpiration to potential evaporation, as the ratio between transpiration and potential evaporation not only varies with stomatal resistance, but also with wind speed, air temperature, irradiance and relative humidity. Furthermore, the effect of wind speed in particular implies increase in potential evaporation, which is commonly interpreted as increased "water stress", but at the same time can reduce leaf transpiration, implying a decrease in water demand at leaf scale.

1 Introduction

Potential evaporation is a measure for atmospheric water demand, i.e. how much water can be evaporated from a wet surface under given atmospheric conditions. The concept of potential evaporation is used commonly in catchment and water balance studies to estimate actual evapotranspiration (McMahon et al., 2013), an important hydrologic pathway of water out of a catchment beside drainage and runoff. Therefore, sensitivity of potential evaporation to changes in atmospheric conditions is generally assumed to scale into sensitivity of actual evapotranspiration and hence catchment water balance (Barella-Ortiz et al., 2013). Similar to actual evapotranspiration in hydrology, the latent heat flux is commonly estimated in global circulation models (GCM) by multiplying potential evaporation by a reduction factor representing water supply limitation to the surface (Milly, 1992). However, recent studies have suggested that 60 to 90 % of latent heat flux on land and half of all solar energy absorbed by terrestrial land surfaces can be attributed to transpiration (Jasechko et al., 2013; Schlesinger and Jasechko, 2014). In contrast to evaporation from wet surfaces, transpiration is commonly controlled by plant stomata, which, by gradually opening and closing, impose a varying resistance on the surface-to-air vapour transfer. Despite this fundamental distinction, it is a surprisingly widely adopted assumption that transpiration scales with "atmospheric evaporative demand" or potential evaporation. Recently, Barella-Ortiz et al. (2013) analysed the sensitivity of different formulations of potential evaporation to climate change, and found large differences in climate sensitivities, depending on the processes included in the formulations. They concluded that those formulations that represent the most complete consideration of physical processes contributing to evaporation are most robust and reliable for the characterisation of the impact of climate change on surface processes.

Published by Copernicus Publications on behalf of the International Association of Hydrological Sciences.

Physically based definitions of potential evaporation consider all or a subset of the following atmospheric variables or various transformations their-of:

- sky radiation
- air temperature
- vapour concentration
- wind speed.

All variables except for vapour concentration generally enhance potential evaporation if considered in the formulation, while increasing vapour concentration reduces potential evaporation. Interestingly, it has been pointed out by several researchers a long time ago, that actual transpiration can actually decrease with increasing wind speed under certain conditions (e.g. Raschke, 1958; Mellor et al., 1964; Monteith, 1965; Dixon and Grace, 1984).

Therefore, in the present study, we challenge the assumption that common definitions of potential evaporation provide a meaningful measure for the sensitivity of transpiration to wind speed and potentially other components of atmospheric forcing. The objective of the present study is to analyse how transpiration from a leaf scales with evaporation from a wet surface with similar properties under the same variations of atmospheric conditions.

2 Methods

In order to consider all relevant atmophseric forcing variables explicitly, and to avoid ambiguities between a "reference crop" and an actual plant, we adopt a detailed physically based leaf transpiration and energy balance model published previously (Schymanski et al., 2013) and compare simulated evaporation from wet leaves with simulations of transpiration from leaves with relatively low stomatal conductance ($0.001\,\mathrm{m\,s^{-1}}$), representing water-stressed plants. Wet leaf evaporation is simulated as transpiration from a leaf with infinite stomatal conductance. All simulations are done for 5 cm wide leaves with stomata on one side of the leaf only. In the present study we focus in particular on the sensitivity to wind speed and in a first step evaluate the model using previously published experimental data on the effect of wind speed on transpiration (Dixon and Grace, 1984).

2.1 Summary of leaf transpiration model

The model was described in detail by Schymanski et al. (2013) and will only be summarised here. Relevant closure equations are also provided in the appendix, while the variables and their units respective standard values are described in Table A1.

The leaf energy balance is determined by the dominant energy fluxes between the leaf and its surroundings, including radiative, sensible, and latent energy exchange (linked to mass exchange). In this study we focus on steady-state conditions, in which the energy balance can be written as:

$$R_\mathrm{s} = R_\mathrm{ll} + H_\mathrm{l} + E_\mathrm{l}, \tag{1}$$

where R_s denotes absorbed shortwave radiation, R_ll is the net longwave radiation, i.e. the emitted minus the absorbed, H_l is the sensible heat flux away from the leaf and E_l is the latent heat flux away from the leaf. In the above, extensive variables are defined per unit leaf area. As in Schymanski et al. (2013), this study considers spatially homogeneous planar leaves, i.e. full illumination and a negligible temperature gradient between the two sides of the leaf.

Following Schymanski et al. (2013) and Monteith and Unsworth (2007), the net longwave emission is represented by the difference between blackbody radiation at leaf (T_l) and that at air temperature (T_a):

$$R_\mathrm{ll} = 2\sigma(T_\mathrm{l}^4 - T_\mathrm{a}^4), \tag{2}$$

where σ is the Stefan-Boltzmann constant and the factor 2 represents the two sides of a broad leaf.

The sensible heat flux or the total convective heat transport away from the leaf is represented as:

$$H_\mathrm{l} = 2h_\mathrm{c}(T_\mathrm{l} - T_\mathrm{a}), \tag{3}$$

where h_c is the average one-sided convective heat transfer coefficient, which depends on leaf size and roughly scales with the square root of wind speed (see Schymanski et al. (2013) for details).

The latent heat flux (E_l) is directly related to the transpiration rate ($E_\mathrm{l,mol}$) by:

$$E_\mathrm{l} = E_\mathrm{l,mol} M_\mathrm{w} \lambda_E, \tag{4}$$

where M_w is the molar mass of water and λ_E the latent heat of vaporisation. $E_\mathrm{l,mol}$ ($\mathrm{mol\,m^{-2}\,s^{-1}}$) was computed in molar units as a function of the concentration of water vapour inside the leaf (C_wl, $\mathrm{mol\,m^{-3}}$) and in the free air (C_wa, $\mathrm{mol\,m^{-3}}$) (Incropera et al., 2006, Eq. 6.8):

$$E_\mathrm{l,mol} = g_\mathrm{tv}(C_\mathrm{wl} - C_\mathrm{wa}), \tag{5}$$

where g_tv ($\mathrm{m\,s^{-1}}$) is the total leaf conductance for water vapour, depending on the leaf boundary layer and stomatal conductance (g_bv and g_sv respectively):

$$g_\mathrm{tv} = \frac{g_\mathrm{bv} g_\mathrm{sv}}{(g_\mathrm{bv} + g_\mathrm{sv})}. \tag{6}$$

Due to their reliance on leaf boundary layer properties, the one-sided heat transfer coefficient (h_c) and the mass transfer coefficient for water vapour (g_bv) across the leaf boundary layer are directly related and both scale roughly with the square root of wind speed (see Appendix A for details). Note

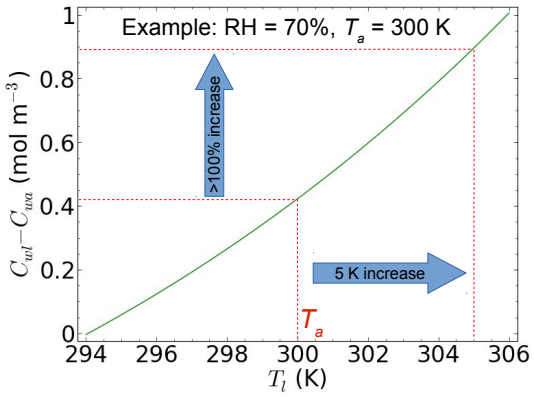

Figure 1. Dependence of the leaf-air water vapour concentration difference ($C_{wl} - C_{wa}$) on leaf temperature (T_l). In this example (70 % relative humidity, 300 K air temperature (T_a)), the water vapour concentration difference doubles for an increase in leaf temperature by 5 K relative to air temperature, or drops to 0 for a decrease in leaf temperature by 6 K.

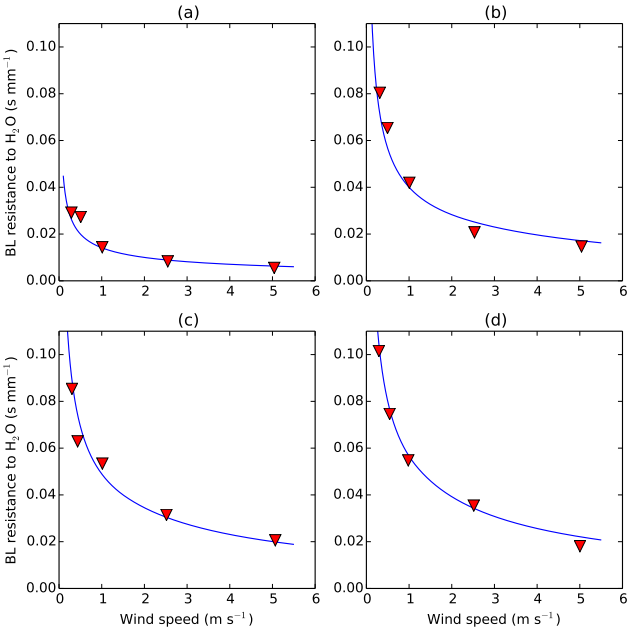

Figure 2. Modelled leaf boundary layer resistance compared to observations by Dixon and Grace (1984). Lines represent inverse of boundary layer conductance (Eqs. A1, A4 and A7), converted to the same units as in Dixon and Grace (1984). Characteristic length scales of leaves (L_l) are chosen to achieve closest match with dots extracted from Fig. 1 in Dixon and Grace (1984). **(a)** *P. sylvestris* ($L_l = 0.0025$ m); **(b)** *S. aucuparia* ($L_l = 0.02$ m); **(c)** *Q. robur* ($L_l = 0.03$ m); **(d)** *F. sylvatica* ($L_l = 0.04$ m).

that the dependence of the leaf-air water vapour concentration difference ($C_{wl} - C_{wa}$) is very sensitive to leaf temperature. For example if the leaf temperature increases by 5 K relative to air temperature, $C_{wl} - C_{wa}$ would double, while if leaf temperature decreased by 6 K, the water vapour concentration difference $C_{wl} - C_{wa}$ would go to 0 at 70 % relative humidity.

For given atmospheric forcing including shortwave irradiance (R_s), water vapour concentration (C_{wa}), temperature (T_a) and wind speed (v_w), the system of equations (see also Appendix A, B and C) is solved numerically for steady state leaf temperature (T_l), returning steady-state values of leaf temperature, net longwave radiation, latent heat flux and sensible heat flux for given leaf size and stomatal conductance.

3 Results

3.1 Model evaluation

Dixon and Grace (1984) placed different plants in a wind tunnel and recorded transpiration rates and leaf temperatures at various wind speeds. To deduce variations in stomatal conductance from the measurements, they also estimated leaf boundary layer resistances for each species using brass leaf replicas. These are plotted in Fig. 2 and we fitted the characteristic leaf length scale in order to reproduce these measurments as close as possible. The resulting characteristic length scales resemble typical leaf widths of these species very closely, with 2.5 mm for pine (*Pinus sylvestris*), 2 cm for mountain-ash (*Sorbus aucuparia*), 3 cm for oak (*Quercus robur*) and 4 cm for beech (*Fagus sylvatica*), while observed and simulated boundary layer resistances match very closely (Fig. 2).

The experimental conditions were reported as 70–75 % relative humidity and 100–200 W m^{-2} absorbed net radiation. Taking a relative humidity of 70 %, assuming that the wind tunnel experiments were conducted under the same air temperature as the growth conditions of the plants (20 °C), and taking into account the ranges of stomatal conductances estimated by Dixon and Grace (1984), we simulated the responses of latent heat flux and leaf temperatures of the different species to variations in wind speed by choosing constant values for absorbed shortwave radiation (R_s) and stomatal conductance (g_{sv}) to best represent the data points in the original study (Fig. 3 in Dixon and Grace, 1984). The results are given in Fig. 3 and the values chosen for R_s and g_{sv} are reported in the figure caption. Our simulations predicted a decrease in both latent heat flux and leaf temperature for all experiments, which is consistent with the experimental results, except for *P. sylvestris*, where an initial increase in transpiration was observed, followed by a decrease at higher wind speeds. Simulated leaf temperatures were generally higher than observed and the discrepancy increased with increasing wind speed.

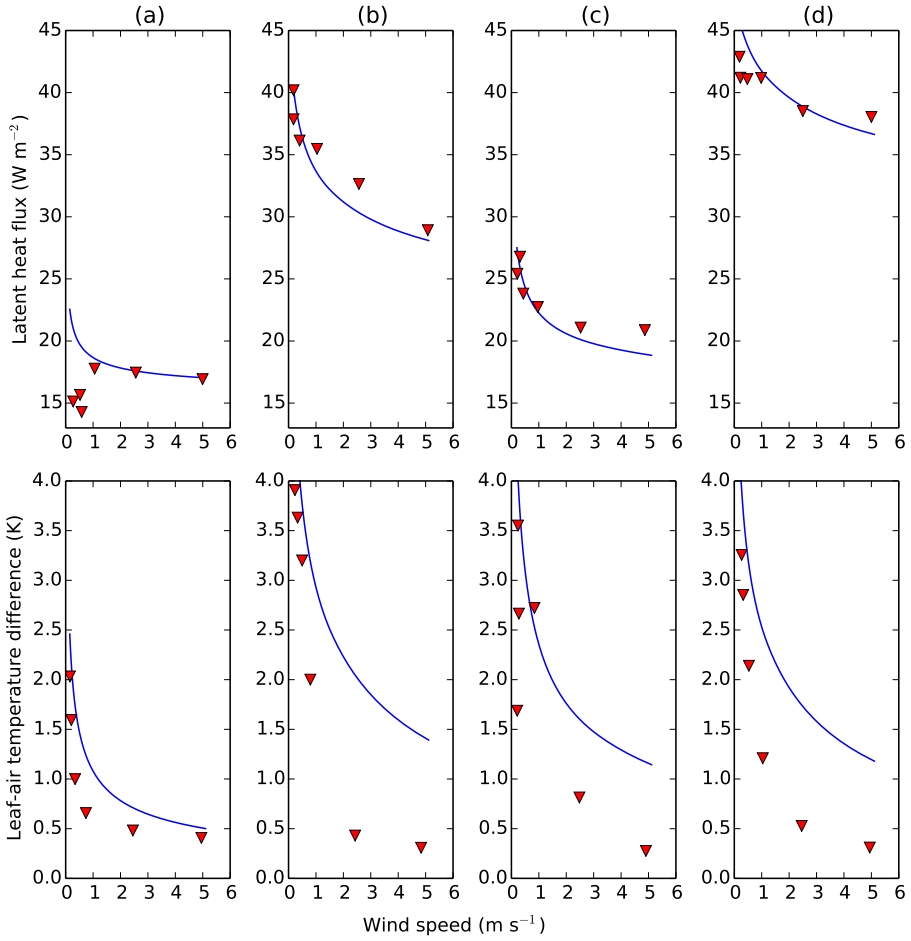

Figure 3. Modelled latent heat fluxes and leaf temperatures compared to observations by Dixon and Grace (1984). Symbols represent data points extracted from Fig. 3 in Dixon and Grace (1984), converted to units used in the present paper. Absorbed shortwave radiation (R_S) and stomatal conductance (g_{sv}) were adapted within the ranges quoted in the paper to best reproduce the data. **(a)** *P. sylvestris* ($R_S = 200\,W\,m^{-2}$, $g_{sv} = 0.00125\,m\,s^{-1}$);**(b)** *S. aucuparia* ($R_S = 200\,W\,m^{-2}$, $g_{sv} = 0.00182\,m\,s^{-1}$); **(c)** *Q. robur* ($R_S = 200\,W\,m^{-2}$, $g_{sv} = 0.00125\,m\,s^{-1}$); **(d)** *F. sylvatica* ($R_S = 170\,W\,m^{-2}$, $g_{sv} = 0.0025\,m\,s^{-1}$).

3.1.1 Simulations of relative evaporation

In order to evaluate the effect of stomatal conductance on the transpiration rate under various conditions, we plotted relative transpiration rates, i.e. transpiration rate at low stomatal conductance ($g_{sv} = 0.001\,m\,s^{-1}$, close to those reported by Dixon and Grace, 1984) divided by transpiration at infinite stomatal conductance as functions of wind speed, shortwave irradiance, relative humidity and air temperature (Fig. 4). Our results illustrate a high sensitivity of relative transpiration to wind speed, with a 3-fold decrease for an increase in wind speed from 0.5 to 5.0 m s^{-1} and weaker, positive sensitivities to shortwave irradiance, relative humidity and air temperature.

4 Discussion

Model simulations and predictions of a decrease in transpiration rates with increasing wind speed were consistent with the experimental results presented by Dixon and Grace (1984). The fact that simulated leaf temperatures were generally higher than the observed and that the discrepancy increased with increasing wind speed is not surprising, considering that temperatures recorded using thermocouples in contact with the leaf surface are influenced by the air passing over the thermocouple (Mott and Peak, 2011), and assuming that this influence increases with increasing wind speed. Note that the simulations in Fig. 3 are performed using constant stomatal conductance, whereas stomatal conductances have likely varied to some extent during the experiments by Dixon and Grace (1984). Considering these uncertainties, the correspondence between observations and model simulations gives us some confidence that the model simulations do rep-

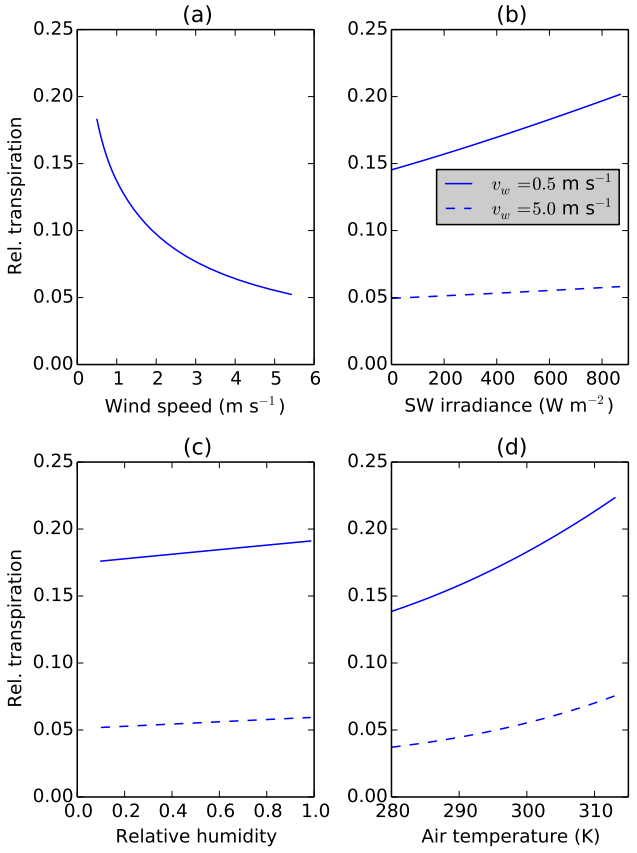

Figure 4. Simulated relative transpiration (latent heat flux at low stomatal conductance (0.001 m s^{-1}) divided by that at infinite stomatal conductance as functions of **(a)** wind speed, **(b)** shortwave irradiance, **(c)** relative humidity and **(d)** air temperature. **(b)**–**(c)** display two curves, one for low wind speed ($v_w = 0.5\,m\,s^{-1}$, solid line) and one for high wind speed ($v_w = 5.0\,m\,s^{-1}$, dashed line). Standard simulation conditions: 5 cm wide leaf, 600 W m^{-2} shortwave irradiance, 300 K air temperature and 50 % relative humidity.

resent the dominant physical processes determining the leaf energy balance.

The analogy with the representation of actual evapotranspiration as a fraction of potential evaporation, in which the reduction coefficient represents soil moisture limitations, is equivalent to assuming that the ratio between potential and actual evapotranspiration is constant as long as surface properties do not change. Figure 4 clearly illustrates that this analogy is inappropriate for plant leaves, particularly with respect to variations in wind speed. At low stomatal conductance, the sensitivity of transpiration to wind speed can even have a different direction than that of potential evapotranspiration, as illustrated in the experimental results, where transpiration decreased with increasing wind speeds. This is of particular relevance for plants in water-limited environments, as higher wind speeds may mean that they can achieve the same amount of carbon assimilation with less water use, indicating more favourable conditions for growth, despite increased potential evaporation. Considering transpiration as a result of a trade-off between water loss and CO_2 uptake, it is also evident that increased solar radiation does not always translate to increased water stress despite its positive effect on potential evaporation. Since solar radiation supplies the energy for photosynthesis and CO_2 assimilation, greater radiation levels enable greater rates of photosynthesis, and hence an environment with a given potential evaporation under high radiation is much more favourable to a plant than an environment with the same potential evaporation under low solar radiation (e.g. wet tropics vs. cold desert). Consideration of the leaf energy balance in the assessment of possible impacts of climate change on vegetation water use and productivity can lead to very different results than if the effect of atmospheric forcing is summarised in the magnitude of "atmospheric water demand" or "potential evaporation". In a related study (Schymanski and Or, 2015), we found that the documented global decrease in wind speeds over land areas (McVicar et al., 2012) may have led to a similarly strong effect on water use efficiency as the rise of atmospheric CO_2 concentrations (Battipaglia et al., 2013; De Kauwe et al., 2013; Barton et al., 2012), but in the opposite direction, implying increase in leaf-scale water use by a similar amount as the decrease expected due to rising CO_2 concentrations (Drake et al., 1997; Gedney et al., 2006; Betts et al., 2007; Gopalakrishnan et al., 2011). In contrast, the effect of decreasing wind speeds on potential evaporation would suggest a general decrease in evaporation and accordingly, increase in streamflow in energy-limited catchments (McVicar et al., 2012).

5 Conclusions

The use of potential evaporation to estimate actual evapotranspiration or to describe the suitability of a given climate for plant growth confounds different effects of atmospheric drivers on transpiration from plant leaves versus evaporation from wet surfaces and may lead to wrong conclusions about the consequences of climate change on plant growth and water relations. This is most pronounced for effects of wind speed, which increases potential evaporation, but may reduce actual transpiration. Therefore, we recommend to avoid using the concept of potential evaporation in relation to plants and transpiration from leaves, and rather address the effects of different atmospheric drivers on plant water use separately.

Appendix A: Leaf conductances to heat and water vapour transfer

The heat transfer coefficient (h_c) for a flat plate can be determined using the non-dimensional Nusselt number (N_{Nu_L}):

$$h_c = k_a \frac{N_{Nu_L}}{L_l}, \tag{A1}$$

where k_a is the thermal conductivity of the air in the boundary layer and L_l is a characteristic length scale of the leaf.

For sufficiently high wind speeds, inertial forces drive the convective heat transport (forced convection) and the relevant dimensionless number is the Reynolds number (N_{Re_L}), which defines the balance between inertial and viscous forces (Incropera et al., 2006, Eq. 6.41):

$$N_{Re_L} = \frac{v_w L_l}{\nu_a}, \tag{A2}$$

where v_w is the wind velocity ($m\,s^{-1}$), ν_a is the kinematic viscosity of the air and L_l is taken as the length of the leaf in wind direction.

In the absence of wind, buoyancy forces, driven by the density gradient between the air at the surface of the leaf and the free air dominate convective heat exchange ("free" or "natural convection"). The relevant dimensionless number here is the Grashof number (N_{Gr_L}), which defines the balance between buoyancy and viscous forces (Incropera et al., 2006, Eqs. 9.3 and 9.65):

$$N_{Gr_L} = \frac{g(\frac{\rho_a - \rho_l}{\rho_l})L_l^3}{\nu_a^2}, \tag{A3}$$

where g is gravity, while ρ_a and ρ_l are the densities of the gas in the atmosphere and at the leaf surface respectively.

For $N_{Gr_L} \ll N_{Re_L}^2$, forced convection is dominant and free convection can be neglected, whereas for $N_{Gr_L} \gg N_{Re_L}^2$ free convection is dominant and forced convection can be neglected (Incropera et al., 2006, p. 565). For simplicity, our numerical experiments were performed under forced conditions, which was satisfied by considering wind speeds greater than $0.5\,m\,s^{-1}$ for 5×5 cm leaves.

The average Nusselt number under forced convection was calculated as a function of the average Reynolds number and a critical Reynolds number (N_{Re_c}) that determines the onset of turbulence and depends on the level of turbulence in the free air stream or leaf surface properties (Incropera et al., 2006, p. 412)

$$N_{Nu_L} = (0.037 N_{Re_L}^{4/5} - C_1) N_{Pr}^{1/3} \tag{A4}$$

with

$$C_1 = 0.037 C_2^{4/5} - 0.664 C_2^{1/2} \tag{A5}$$

and

$$C_2 = \frac{N_{Re_L} + N_{Re_c} - |N_{Re_c} - N_{Re_L}|}{2}. \tag{A6}$$

Equation (A6) was introduced to make Eq. (A4) valid for all Reynolds numbers, and following considerations by Schymanski et al. (2013), we chose $N_{Re_c} = 3000$ in the present simulations.

Due to their reliance on leaf boundary layer properties, the heat transfer coefficient (h_c) and the mass transfer coefficient for water vapour (g_{bv}) across the leaf boundary layer are directly related (Incropera et al., 2006, Eq. 6.60):

$$g_{bv} = \frac{a_s h_c}{\rho_a c_{pa} N_{Le}^{1-n}}, \tag{A7}$$

where a_s is the fraction of transpiring surface area in relation to the surface area for sensible heat exchange (e.g. 0.5 if stomata are on one side of the leaf only), c_{pa} is the constant-pressure heat capacity of air, n is an empirical constant ($n = 1/3$ for general purposes) and N_{Le} is the dimensionless Lewis number, defined as (Incropera et al., 2006, Eq. 6.57):

$$N_{Le} = \alpha_a / D_{wa}, \tag{A8}$$

where α_a is the thermal diffusivity of air.

The heat and mass transfer coefficients described above can be seen as the reciprocals of flow resistances, $1/g_{bv}$ representing the boundary layer resistance for water vapour transfer. For transpiration through stomata, we have to consider the additional stomatal resistance ($1/g_{sv}$), so that the total leaf conductance to water vapour becomes:

$$\frac{1}{g_{tv}} = \frac{1}{g_{bv}} + \frac{1}{g_{sv}}, \tag{A9}$$

resulting in Schymanski et al. (2013):

$$g_{tv} = \frac{g_{bv} g_{sv}}{(g_{bv} + g_{sv})}. \tag{A10}$$

Appendix B: Effect of leaf temperature on the leaf-air vapour concentration gradient

The concentration difference in Eq. (5) is a function of the temperature and the vapour pressure differences between the leaf and the free air. Assuming that water vapour behaves like an ideal gas, we can express its concentration as:

$$C_{wl} = \frac{P_{wl}}{R_{mol} T_l}, \tag{B1}$$

where P_{wl} is the vapour pressure inside the leaf, R_{mol} is the universal gas constant and T_l is leaf temperature. In this study the vapour pressure inside the leaf is assumed to be the saturation vapour pressure at leaf temperature, which is computed using the Clausius-Clapeyron relation (Eq. (B.3) in Hartmann, 1994):

$$P_{wl} = 611 \exp\left(\frac{\lambda_E M_w}{R_{mol}}\left(\frac{1}{273} - \frac{1}{T_l}\right)\right), \tag{B2}$$

where λ_E is the latent heat of vaporisation and M_w is the molar mass of water.

Table A1. Symbols, standard values and units used in this paper. All area-related variables are expressed per unit leaf area.

Symbol	Description (standard value)	Units
α_a	Thermal diffusivity of air	$m^2\,s^{-1}$
λ_E	Latent heat of vaporisation (2.45×10^6)	$J\,kg^{-1}$
ν_a	Kinematic viscosity of air	$m^2\,s^{-1}$
ρ_a	Density of dry air	$kg\,m^{-3}$
σ	Stefan-Boltzmann constant (5.67×10^{-8})	$W\,m^{-2}\,K^{-4}$
a_s	Fraction of transpiring leaf surface area (1/2 for hypostomatous leaves)	-
C_{wa}	Concentration of water vapour in the free air	$mol\,m^{-3}$
C_{wl}	Concentration of water vapour inside the leaf	$mol\,m^{-3}$
c_{pa}	Specific heat of dry air (1010)	$J\,K^{-1}\,kg^{-1}$
D_{wa}	Binary diffusion coefficient of water vapour in air	$m^2\,s^{-1}$
E_l	Latent heat flux away from leaf	$W\,m^{-2}$
$E_{l,mol}$	Transpiration rate in molar units	$mol\,m^{-2}\,s^{-1}$
g_{bv}	Leaf boundary layer conductance to water vapour	$m\,s^{-1}$
g_{sv}	Stomatal conductance to water vapour	$m\,s^{-1}$
g_{tv}	Total leaf conductance to water vapour	$m\,s^{-1}$
h_c	Average convective heat transport coefficient for the whole leaf	$W\,m^{-2}\,K^{-1}$
H_l	Sensible heat flux emitted by the leaf	$W\,m^{-2}$
k_a	Thermal conductivity of air in leaf boundary layer	$W\,m^{-1}\,K^{-1}$
L_l	Characteristic leaf length scale	m
m_w	Leaf water content	$kg\,m^{-2}$
M_w	Molar mass of water (0.018)	$kg\,mol^{-1}$
n_a	Amount of matter	mol
N_{Le}	Lewis number	–
N_{Nu}	Nusselt number	–
N_{Nu_L}	Average Nusselt number for whole leaf	–
N_{Pr}	Prandtl number for air (0.71)	–
N_{Re_c}	Critical Reynolds number (3000)	–
N_{Re_L}	Average Reynolds number for whole leaf	–
P_{wa}	Vapour pressure in free air	Pa
P_{wl}	Vapour pressure inside the leaf	Pa
R_{mol}	Molar gas constant (8.314472)	$J\,K^{-1}\,mol^{-1}$
R_s	Absorbed shortwave radiation	$W\,m^{-2}$
R_{ll}	Net longwave radiation emission by a leaf	$W\,m^{-2}$
T_a	Air temperature	K
T_l	Leaf temperature	K
v_w	Wind velocity	$m\,s^{-1}$

Appendix C: Model closure

In order to simulate steady state leaf temperatures and the leaf energy balance terms using the above equations, it is necessary to calculate ρ_a, D_{wa}, α_a, k_a, and ν_a, while L_l, Re_c and g_{sv} are input parameters, and P_{wa} and v_w (vapour pressure and wind speed) are part of the environmental forcing. D_{wa}, α_a, k_a and ν_a were parameterised as functions of boundary layer temperature (T_b) only, by fitting linear curves to published data (Monteith and Unsworth, 2007, Table A.3):

$$D_{wa} = (1.49 \times 10^{-7})T_b - 1.96 \times 10^{-5} \quad \text{(C1)}$$

$$\alpha_a = (1.32 \times 10^{-7})T_b - 1.73 \times 10^{-5} \quad \text{(C2)}$$

$$k_a = (6.84 \times 10^{-5})T_b + 5.62 \times 10^{-3} \quad \text{(C3)}$$

$$\nu_a = (9 \times 10^{-8})T_b - 1.13 \times 10^{-5}, \quad \text{(C4)}$$

where the boundary layer temperature is approximated as:

$$T_b = (T_a + T_l)/2. \quad \text{(C5)}$$

Assuming that air and water vapour behave like an ideal gas, and that dry air is composed of 79 % N_2 and 21 % O_2, we calculated the density as a function of temperature, vapour pressure and the partial pressures of the other two compo-

nents using the ideal gas law:

$$\rho_a = \frac{n_a M_a}{V_a} = M_a \frac{P_a}{R_{mol}, T_a}, \quad \text{(C6)}$$

where n_a is the amount of matter (mol), M_a is the molar mass (kg mol^{-1}), P_a the pressure, T_a the temperature and R_{mol} the molar universal gas constant. This equation was used for each component, i.e. water vapour, N_2 and O_2, where the partial pressures of N_2 and O_2 are calculated from atmospheric pressure minus vapour pressure, yielding:

$$\rho_a = \frac{M_w P_v + M_{N_2} P_{N_2} + M_{O_2} P_{O_2}}{R_{mol} T_a}, \quad \text{(C7)}$$

where M_{N_2} and M_{O_2} are the molar masses of nitrogen and oxygen respectively, while P_{N_2} and P_{O_2} are their partial pressures, calculated as:

$$P_{N_2} = 0.79(P_a - P_{wa}) \quad \text{(C8)}$$

and

$$P_{O_2} = 0.21(P_a - P_{wa}). \quad \text{(C9)}$$

Acknowledgements. The authors are grateful to Francis Chiew for inviting this contribution to the Session "Hydrologic Non-Stationarity and Extrapolating Models to Predict the Future" at the IUGG 2015 General Assembly, and to Jai Vaze and an anonymous reviewer for helpful comments.

References

Barella-Ortiz, A., Polcher, J., Tuzet, A., and Laval, K.: Potential evaporation estimation through an unstressed surface-energy balance and its sensitivity to climate change, Hydrol. Earth Syst. Sci., 17, 4625–4639, doi:10.5194/hess-17-4625-2013, 2013.

Barton, C. V., Duursma, R. A., Medlyn, B. E., Ellsworth, D. S., Eamus, D., Tissue, D. T., Adams, M. A., Conroy, J., Crous, K. Y., Liberloo, M., Löw, M., Linder, S., and McMurtrie, R. E.: Effects of elevated atmospheric [CO_2] on instantaneous transpiration efficiency at leaf and canopy scales in Eucalyptus saligna, Global Change Biol., 18, 585–595, doi:10.1111/j.1365-2486.2011.02526.x, 2012.

Battipaglia, G., Saurer, M., Cherubini, P., Calfapietra, C., McCarthy, H. R., Norby, R. J., and Francesca Cotrufo, M.: Elevated CO_2 increases tree-level intrinsic water use efficiency: insights from carbon and oxygen isotope analyses in tree rings across three forest FACE sites, New Phytol., 197, 544–554, doi:10.1111/nph.12044, 2013.

Betts, R. A., Boucher, O., Collins, M., Cox, P. M., Falloon, P. D., Gedney, N., Hemming, D. L., Huntingford, C., Jones, C. D., Sexton, D. M. H., and Webb, M. J.: Projected increase in continental runoff due to plant responses to increasing carbon dioxide, Nature, 448, 1037–1041, doi:10.1038/nature06045, 2007.

De Kauwe, M. G., Medlyn, B. E., Zaehle, S., Walker, A. P., Dietze, M. C., Hickler, T., Jain, A. K., Luo, Y., Parton, W. J., Prentice, I. C., Smith, B., Thornton, P. E., Wang, S., Wang, Y.-P., Wårlind, D., Weng, E., Crous, K. Y., Ellsworth, D. S., Hanson, P. J., Seok Kim, H., Warren, J. M., Oren, R., and Norby, R. J.: Forest water use and water use efficiency at elevated CO_2: a model-data intercomparison at two contrasting temperate forest FACE sites, Global Change Biol., 19, 1759–1779, doi:10.1111/gcb.12164, 2013.

Dixon, M. and Grace, J.: Effect of wind on the transpiration of young trees, Ann. Botany, 53, 811–819, 984.

Drake, B. G., Gonzàlez-Meler, M. A., and Long, S. P.: More Efficient Plants: A Consequence of Rising Atmospheric CO_2?, Ann. Rev. Plant Physiol. Plant Molec. Biol., 48, 609–639, doi:10.1146/annurev.arplant.48.1.609, 1997.

Gedney, N., Cox, P. M., Betts, R. A., Boucher, O., Huntingford, C., and Stott, P. A.: Detection of a direct carbon dioxide effect in continental river runoff records, Nature, 439, 835–838, 2006.

Gopalakrishnan, R., Bala, G., Jayaraman, M., Cao, L., Nemani, R., and Ravindranath, N. H.: Sensitivity of terrestrial water and energy budgets to CO_2-physiological forcing: an investigation using an offline land model, Environ. Res. Lett., 6, 044013, doi:10.1088/1748-9326/6/4/044013, 2011.

Hartmann, D. L.: Global physical climatology, Academic Press, 1994.

Incropera, F. P., DeWitt, D. P., Bergman, T. L., and Lavine, A. S.: Fundamentals of Heat and Mass Transfer, John Wiley & Sons, 6th edn., 997 pp., 2006.

Jasechko, S., Sharp, Z. D., Gibson, J. J., Birks, S. J., Yi, Y., and Fawcett, P. J.: Terrestrial water fluxes dominated by transpiration, Nature, 496, 347–350, doi:10.1038/nature11983, 2013.

McMahon, T. A., Peel, M. C., Lowe, L., Srikanthan, R., and McVicar, T. R.: Estimating actual, potential, reference crop and pan evaporation using standard meteorological data: a pragmatic synthesis, Hydrol. Earth Syst. Sci., 17, 1331–1363, doi:10.5194/hess-17-1331-2013, 2013.

McVicar, T. R., Roderick, M. L., Donohue, R. J., Li, L. T., Van Niel, T. G., Thomas, A., Grieser, J., Jhajharia, D., Himri, Y., Mahowald, N. M., Mescherskaya, A. V., Kruger, A. C., Rehman, S., and Dinpashoh, Y.: Global review and synthesis of trends in observed terrestrial near-surface wind speeds: Implications for evaporation, J. Hydrol., 416–417, 182–205, doi:10.1016/j.jhydrol.2011.10.024, 2012.

Mellor, R. S., Salisbury, F. B., and Raschke, K.: Leaf temperatures in controlled environments, Planta, 61, 56–72, doi:10.1007/BF01895390, 1964.

Milly, P. C. D.: Potential Evaporation and Soil Moisture in General Circulation Models, Journal of Climate, 5, 209–226, doi:10.1175/1520-0442(1992)005<0209:PEASMI>2.0.CO;2, 1992.

Monteith, J. and Unsworth, M.: Principles of Environmental Physics, Third Edition, Academic Press, 3rd edn., 440 pp., 2007.

Monteith, J. L.: Evaporation and environment, Symposia of the Society for Experimental Biology, 19, 205–234, http://www.ncbi.nlm.nih.gov/pubmed/5321565 (last access: 21 September 2011), 1965.

Mott, K. A. and Peak, D.: Alternative perspective on the control of transpiration by radiation, Proceedings of the National Academy of Sciences, 108, 19820–19823, doi:10.1073/pnas.1113878108, 2011.

Raschke, K.: Über den Einfluß der Diffusionswiderstände auf die Transpiration und die Temperatur eines Blattes, Flora, 146, 546–578, 1958.

Schlesinger, W. H. and Jasechko, S.: Transpiration in the global water cycle, Agr. Forest Meteorol., 189-190, 115–117, doi:10.1016/j.agrformet.2014.01.011, 2014.

Schymanski, S. J. and Or, D.: Surprising effects of wind speed on leaf energy balance, transpiration and water use efficiency, submitted, 2015.

Schymanski, S. J., Or, D., and Zwieniecki, M.: Stomatal Control and Leaf Thermal and Hydraulic Capacitances under Rapid Environmental Fluctuations, PLoS ONE, 8, e54231, doi:10.1371/journal.pone.0054231, 2013.